

1 Colorimetric derivatization of ambient ammonia (NH₃) for detection by 2 long path absorption photometry

3 Shasha Tian^{a, b, 1}, Kexin Zu^{a, b, 1}, Huabin Dong^{a, b, *}, Limin Zeng^{a, b}, Keding Lu^{a, b}, Qi Chen^a

4 ^a State Key Joint Laboratory of Environmental Simulation and Pollution Control, College of
5 Environmental Sciences and Engineering, Peking University, Beijing, 100871, China.

6 ^b International Joint laboratory for Regional pollution Control (IJRC), Peking University, Beijing, China

7 * Corresponding author: hbdong@pku.edu.cn

8
9 **Abstract.** In the last few decades, various techniques, including spectroscopic, mass spectrometric,
10 chemiluminescence, and wet chemical methods, had been developed and applied for the detection of
11 gaseous ammonia (NH₃). We developed an online NH₃ monitoring system—salicylic acid derivatization
12 reaction and long path absorption photometer (SAC-LOPAP)—based on a selective colorimetric reaction
13 to form a highly absorbing reaction product and a LOPAP, which could run stably for a long time and be
14 applied to the continuous online measurement of low concentrations of ambient NH₃ by optimizing the
15 reaction conditions, adding a constant temperature module and liquid flow controller. The detection limit
16 reached with this instrument was 40.5 ppt with a stripping liquid flow rate of 0.49 ml min⁻¹ and a gas
17 sample flow rate of 0.70 L min⁻¹. An inter-comparison of our system with a commercial instrument
18 Picarro G2103 analyzer (Picarro, US) in Beijing was presented, and the results showed that the two
19 instruments had a good correlation with a slope of 1.00 and an R² of 0.96, indicating that the SAC-
20 LOPAP involved in this study could be used for the accurate measurement of NH₃.

21 1. Introduction

22 Gaseous ammonia (NH₃) widely exists in the atmosphere and plays an important role in many
23 atmospheric chemical reactions (Swati and Hait, 2018; Klimczyk et al., 2021; Wang et al., 2018). As the
24 most abundant alkaline gas in the atmosphere, NH₃ easily forms ammonium ions (NH₄⁺) with water and
25 reacts with acidic species to form secondary inorganic particles (Ianniello et al., 2011; Ni et al., 2000).
26 These secondary particles are considered a major source of fine particulate matter (PM), which is harmful
27 to climate, visibility and human health (Bu et al., 2021; Gao et al., 2021). Furthermore, recent studies
28 have shown that NH₃ is necessary to control fine particulate pollution (Wen et al., 2018; Wang et al.,

29 2013). Due to those problems, the inventory of NH₃ emissions and concentration in urban air has been
30 highly evaluated. Agriculture, including animal feedlot operations, is considered as the largest emission
31 source of NH₃ with 80.6% of the global anthropogenic emissions followed by 11% from biomass burning
32 and 8.3% from the energy sector, including industries and traffic (Behera et al., 2013). Expert estimate
33 that global annual emissions of ~~NH₃~~NH₃ will increase from 65 Tg N yr⁻¹ in 2008 to 135 Tg N yr⁻¹ in
34 2100 (Fowler et al., 2015). However, ambient measurement of NH₃ concentrations is difficult due to
35 several factors: ambient levels vary widely with from 5 pptv to 500 ppbv (Janson et al., 2010; Krupa,
36 2003; Sutton et al., 1995). Ammonia exists in gaseous, particulate and liquid phases, which add further
37 complicates the measurement (Warneck, 1988). In addition, NH₃ is “sticky” and interacts with surfaces
38 of materials, resulting in slow inlet response times (Yokelson et al., 2003). Finally, the temperature
39 difference between the indoor and outdoor environments and the humidity difference between the inside
40 and outside of the instrument will reduce the accuracy of measurement and calibration. It is therefore
41 essential to accurately measure ambient NH₃ to better quantify concentration and concentration changes
42 and hence to evaluate the impacts of NH₃.

43 In recent years, researchers have developed techniques and methods for detecting NH₃ in the
44 atmosphere, which include spectroscopic, mass spectrometric, chemiluminescence, and wet chemical
45 methods (Von et al., 2009). Spectroscopic methods, such as Cavity Enhanced Absorption Spectroscopy
46 (CEAS) (Gong et al., 2017; Berden et al., 2000) and Cavity Ring-Down Spectroscopy (CRDS) (Martin
47 et al., 2016; Qu et al., 2012), can greatly improve spectral absorption's effective optical path length by
48 using the optical cavity structure. However, the “sticky” of NH₃ will affect background, detection
49 efficiency and detection response time of the instrument (Whitehead et al., 2008; Yokelson et al., 2003).
50 Utilizing a quantum cascade laser (QCL) or a DFB laser in a near-infrared band as the light source can
51 achieve a low detection limit of 0.018ppb (Whitehead et al., 2008; Mcmanus et al., 2002; Von et al.,
52 2009), realizing the measurement of low concentrations of NH₃ in ambient air. Mass-spectrography
53 analyzers provide highly sensitive techniques but may be less specific and can be affected by competing
54 ion chemistries. The chemical ionization mass spectrometer (CIMS) technique is based on an ion-
55 molecule reaction to selectively ionize and detect trace_NH₃ in the atmosphere, which features a fast
56 response and in situ measurement (Benson et al., 2010; Nowak et al., 2007; Yu and Lee, 2012). It has
57 the advantages of small volume and wide measurement range, but its detection limit is very high (Ajay

58 and Beniwal., 2019). Chemiluminescence is an indirect method to measure ammonia. Two catalytic
59 converters of different characteristics catalyze NO_x and NO-amine into NO. The NH₃ ~~mining-mixing~~
60 ratio is calculated by the difference between NO_x and NO-amine. This method can realize the
61 simultaneous measurement of NH₃, NO and NO₂, but the measurement results are affected by the
62 conversion efficiency (Sharma et al., 2010; Sharma et al., 2012). Wet chemistry methods convert gas-
63 phase NH₃ to aqueous NH₃ (NH₄⁺) for online analysis by means of online ion chromatography with a
64 detection limit of 0.05 μg m⁻³ (0.72ppb at 25 °C) (Khlystov et al., 1995; Dong et al., 2012; Makkonen
65 et al., 2012). A field inter-comparison of NH₃ measurement techniques found that wet chemistry
66 instruments showed better long-term stability and agreement than other analyzers (Von et al., 2009),
67 which was due to the wet chemical trapping method and standard calibration solutions, humidity did not
68 affect the measurement, and the standard solution was more stable than standard gases. However, they
69 failed to capture the peak because of lower time resolution. Based on a selective colorimetric reaction to
70 form a highly absorbing reaction product and absorption spectrophotometry collect NH₃ (and ammonium)
71 by aqueous scrubbing in glass frit impactors (Bianchi et al., 2012; Bae et al., 2007) has been used for
72 decades for routine derivatization and colorimetric analysis of NH₄⁺ in a wide variety of environmental
73 samples (e.g. soils, environmental waters, etc), which has also been reported by other scholars (Bae et
74 al., 2007). In those studies the product was detected by a long-path absorption photometer (LOPAP), in
75 which the absorbance of the solution is amplified in the long-+ path module to reach a lower detection
76 limit (Heland et al., 2001).

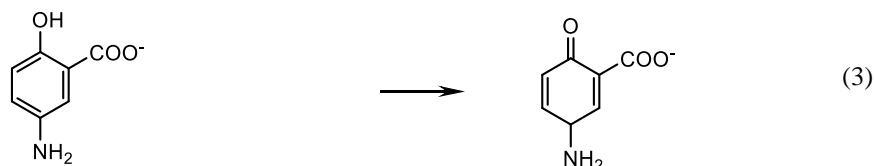
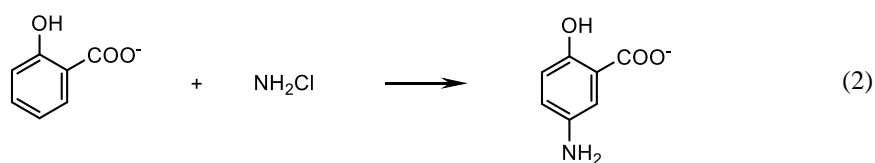
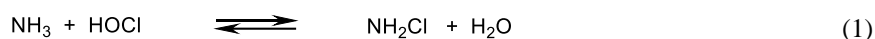
77 In this study, we provide an online NH₃ monitoring system based on wet chemistry stripping of
78 atmospheric NH₃, followed by the formation of a highly light-absorbing indophenol after a salicylic acid
79 derivatization reaction to produce the colored reaction product reaction and detected with LOPAP.
80 According to Lambert-Beer's law, the sensitivity of spectrophotometry can be enhanced by increasing
81 the optical path length. This sensitive analytical method has already been successfully applied in different
82 colorimetric detection studies (Yao et al., 1998; Heland et al., 2001; Callahan et al., 2002). In analogy to
83 the original long path absorption photometer (LOPAP) which was developed for HONO measurements
84 (Kleffmann et al., 2002), we call this monitoring system the salicylic acid derivatization reaction and
85 long path absorption photometer (SAC-LOPAP), which features several improvements over versions
86 previously reported by other groups: one is the optimization of reaction conditions, the other

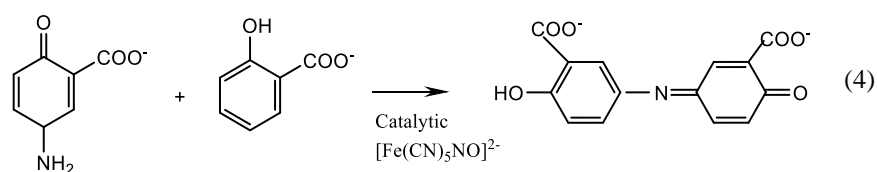
87 modification is the use of constant temperature module and flow control system. Secondly, we will
88 present measurements demonstrating our new system in urban environments in Peking University, with
89 measure low concentrations, good stability and low detection limit.

90 2. SAC-LOPAP instrument

91 2.1 Measurement principle

92 Our instrument is designed to measure NH_3 in a low-concentration environment (under 20ppb) with the
93 good stability, low detection limit (less than 60 ppt) and small size. There is a brief introduction to the
94 principle of the instrument. The measurement of NH_3 in the SAC-LOPAP instrument is achieved by the
95 selective colorimetric reaction to form a highly absorbing reaction product and absorption
96 spectrophotometry. Samples containing dissolved ammonia and ammonium react with a phenolic
97 compound and a chlorine-donating reagent to form indophenol blue during the reaction, with the
98 strongest absorption at a wavelength of 665 nm. (Krom and Michael, 1980; Searle and Phillip, 1984).The
99 reaction mechanism of the chromogenic reactions as shown in (1)-(4). Furthermore, to measure the
100 absorbance of the sample, we used a LOPAP based on liquid-waveguide capillary cell (LWCC)
101 technology to obtain a better detection limit, continuity and stability (Heland et al., 2001).





102 2.2 Experiment setup

103 We designed our system to consist of four modules: the sampling module, the reacting module, the
 104 detecting module, and the control module (Fig. 1). The key component of the sampling module is a glass
 105 coil reactor, which is an open glass tube (inner diameter 1.5 mm, 75 cm long) coiled 12 turns. At the
 106 beginning of this coil, there is a flow manifold to mix the ambient air flow and the stripping solutions.
 107 The air is pumped into the stripping coil under the action of a vacuum diaphragm air pump and a gas
 108 flow meter (Horiba, China) (Chen et al., 2004). To protect the gas flowmeter and the air pump, a security
 109 bottle is installed in front of the gas flowmeter to prevent the inflow of liquid. At the same time, the
 110 stripping solution, regulated by the liquid flow control system, is injected into the stripping coil to capture
 111 NH_3 in the air and form a mixture of ammonium-salicylic acid. To achieve higher absorption efficiency,
 112 circulating cooling water with a temperature of 10-15 °C is provided outside the stripping coil. The center
 113 part of the reacting module is a reaction coil and a debubble. The liquid sample is mixed with the alkaline
 114 derivatization solution, and a derivatization reaction to produce the colored reaction product reaction
 115 occurs in the heated reaction coil. The reaction coil is made of a 90 cm length of Teflon tubes coiled on
 116 a heat-conducting metal cylinder, and a PID controller controls the temperature of the reactor at 40-75
 117 °C to accelerate the derivatization reaction. After the derivatization reaction, the sample is sent to the
 118 detecting module, which comprises a liquid waveguide capillary cell (LWCC-100, World Precision
 119 Instruments, USA) with optical path length of 100 cm, an LED light source with the mode at 665 nm
 120 (Ocean Optics) and a phototube (S16008-33, HAMAMTSU, Japan) for the long path photometry
 121 detection. The sample solution to be tested is filtered by a 1.0 μm filter before passing through LWCC to
 122 avoid interference from components of the sample matrix/method reagents. Both the fluid propulsion
 123 module and detection module can be computer controlled.

124 Eq. (5) can help convert the concentration of NH_4^+ solution $C_{\text{NH}_4^+}$ to the NH_3 concentration in the
 125 gaseous C_{NH_3} .

$$C_{NH_3} = \frac{c_{NH_4^+} F_l RT}{M_{NH_4^+} M_{NH_3} F_g P \gamma} \quad (5)$$

Where C_{NH_3} denotes the content of NH_3 in the air sample (ppb), P denotes atmospheric pressure (101.3 kPa), $M_{NH_4^+} M_{NH_3}$ denotes the molar mass of NH_3 (18.0417 g/mol), $R=8.314 \text{ Pa} \cdot \text{m}^3 \cdot \text{mol}^{-1} \cdot \text{K}^{-1}$. T denotes the room temperature (K), F_l denotes the flow rate of stripping solution, F_g denotes the flow rate of sampling gas, γ denotes the capture efficiency of air NH_3 in the stripping solution (a constant determined by laboratory).

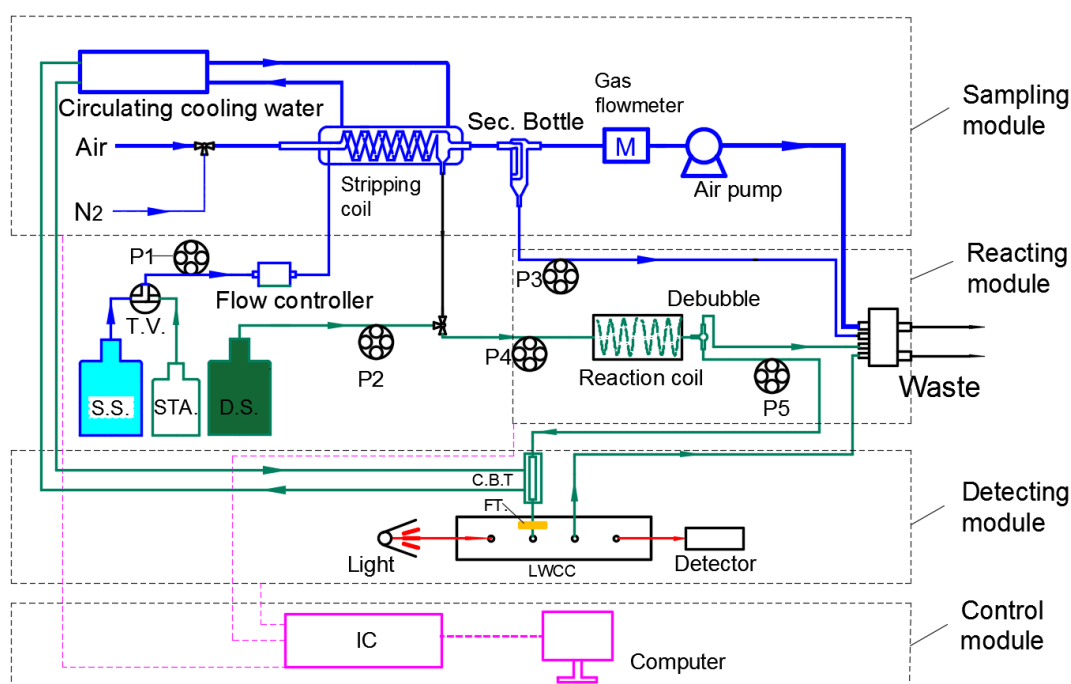


Fig. 1. Schematic diagram of SAC-LOPAP. (M: gas flowmeter; S.S.: stripping solution; STA.: standard solution; D.S.: derivatization solution; Sec. Bottle: security bottle; C.B.T: cooling buffer tube; T.V.: triple valve for switching stripping solution and standard solution; P1, P2, P3, P4, P5: peristaltic pump for transferring solutions; FT: syringe filter; IC: integrated circuit. The gas flow rate can be controlled from 0.2-2.0 L min^{-1} , with an optimal gas flow rate of 0.7 L min^{-1} . The liquid flow rate can be controlled from 0.1-1.0 ml min^{-1} , with an optimal stripping liquid flow rate of 0.49 ml min^{-1}).

2.3 Experiment protocol

The exact recipe of the chemical reactions follows the reactions described by Searle et al (Searle and Phillip, 1984). We used 0.75 g L^{-1} salicylic acid (TCI, 99.5%, Japan), 0.014 g L^{-1} sodium nitroferricyanide

142 (TCI, 99%, Japan), and 0.2 g L⁻¹ NaOH as stripping solution (R1). Then the 0.188ml L⁻¹ Sodium
143 hypochlorite (Aladdin, active chlorine 10%, China) and 1.5 g L⁻¹ NaOH as derivatization solution (R2).
144 We acknowledge that based on a selective colorimetric reaction to form a highly absorbing reaction
145 product must be carried out under catalytic and alkaline conditions. Sodium nitroferricyanide is
146 recognized as a high-efficiency catalytic to increase the sensitivity of the Equation 4 (Krom and Michael,
147 1980; Searle and Phillip, 1984).

148 Calibrating the setup uses NH₄⁺ standard solution produced by the National Institute of Metrology,
149 China. The standards are prepared shortly before use by NH₄⁺ standard solution with R1 in volumetric
150 bottle and to use it right after it was ready. The ideal use cycle of R1 and R2 was half a month. ~~After~~
151 after replacement with new R1 and R2 solutions and other instrument fittings, the instrument should be
152 recalibrated to ensure data quality.

153 2.4 Sampling method

154 The inter-comparison experiment was conducted at the College of Environment Sciences and
155 Engineering, Peking University, located within the 4th ring road in northern Beijing, China (39.59° N,
156 116.18°E). A commercial instrument Picarro G2103 analyzer (Picarro, US) used for atmospheric NH₃
157 measurement based on the CRDS method was deployed concurrently with SAC-LOPAP in the
158 comparison, which could be used to validate other instruments (Twigg et al., 2022). The experiment took
159 place from 15 September 2021 to 15 October 2021, with the instruments installed in a field container.
160 Two instruments shared an inlet and were deployed 2.5 m above the ground. A Polytetrafluoroethylene
161 (PTFE) filter (46.2 mm diameter, 2 μm pore size, Whatman, USA) is used in the front of the sample
162 module to remove ambient aerosols, which is placed into a round filter holder made of perfluoro alkoxy
163 (PFA). We changed the filter every day with the aim of avoiding uncertainties. After the filtration of the
164 aerosols, the sample gas flow is delivered into a 3.8 m long 1/4-inch Teflon tube, and a temperature-
165 controlled metal heating wire (set at 35 °C ±0.1 °C) is wrapped around the sample tube and covered with
166 thermo-isolation materials. We ran our instrument with an additional drag flow of 1.75 L min⁻¹ with aim
167 to ensure the ambient residence time was about 7.8 msec for all instruments. Data acquisition times were
168 different for the above instruments during the inter-comparison. The base reporting periods for Picarro
169 and SAC-LOPAP were 1 s and 30 s. For the purposes of comparison, data from the two instruments

170 presented in this section were averaged to 30 s. In addition, high purity N₂ as zero gas was injected into
171 the sampling tube and carried out every 7 days at the start and end of the campaign as well. The standard
172 air source comes from China Sichuan Zhongce Biaowu Technology Co., LTD. The quality management
173 system of the company conforms to the recognized standard in the Chinese industry (GB/T9001-
174 2016/ISO 9001:2015). The composition was ammonia (5.08 ppm) and nitrogen with the uncertainty was
175 2%. In the test, pure N₂ was used as the dilution gas to obtain the required concentration of ammonia
176 standard gas. Calibrations were performed using combinations of concentrations at 1.32, 4.95, 9.59,
177 17.90 and 54.96 ppb from the cylinder. In addition, 4.95 ppb and 54.96 ppb standard gas were injected
178 into the sample tube every 7 days after zero point. The field container was controlled at 25 °C ±1 °C to
179 reduce the impact of temperature fluctuations on measurement results.

180 **3 Characterization and optimization**

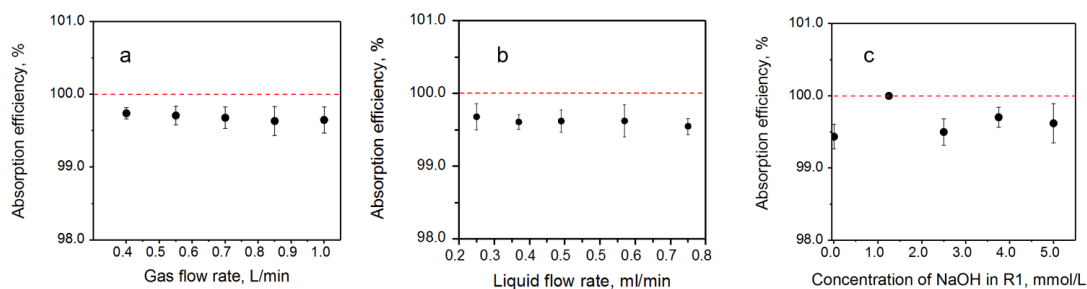
181 **3.1 Sampling efficiency**

182 NH₃ Standard gas of 54.96 ppb was used as the sample to be collected through two identical serial
183 stripping coils, and the concentration of liquid samples collected by the two stripping coils was measured
184 to calculate the capture efficiency. The calculation formula is as below.

$$185 \quad \gamma_1 = \frac{c_1}{c_1+c_2} \times 100\% \quad (6)$$

186 Where, γ_1 denotes the collection efficiency of the first stripping coil, c_1 and c_2 denote the concentration
187 of NH₄⁺ trapped in the first stripping coil and the second stripping coil, respectively.

188 The collection efficiency of NH₃ from the R1 reached more than 99% under different c_{NaOH} , F_l , and
189 F_g . Figure 2a and Figure 2b show that the F_l and the F_g had almost no influence on collection efficiency.
190 Figure 2c shows that c_{NaOH} of 1.25 mmol L⁻¹ achieved the greatest collection efficiency in the R1 (99.9%).
191 Therefore, the c_{NaOH} of 1.25 mmol L⁻¹ was selected as the R1 of the NH₃. And we selected F_l as 0.49 ml
192 min⁻¹ and F_g as 0.7 L min⁻¹ in order to achieve the required detection range in this study.



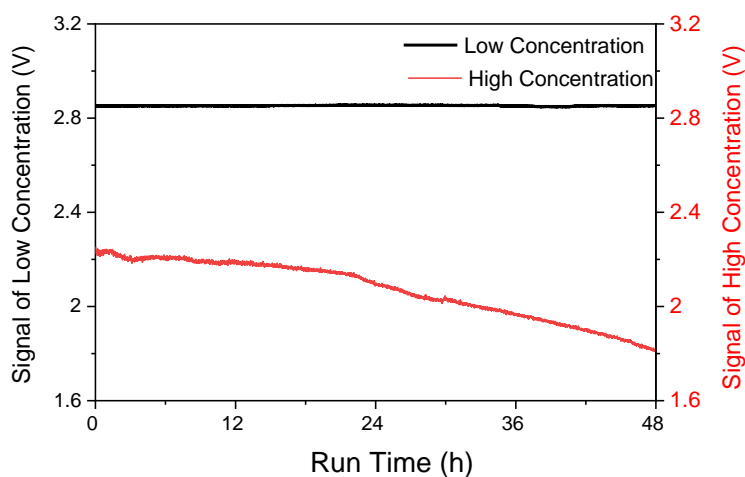
193

194 Fig. 2. The absorption efficiency of stripping coil versus (a) gas flow rate ($C_{NaOH} = 4.0 \text{ mmol L}^{-1}$, $F_l = 0.49 \text{ ml min}^{-1}$),
 195 (b) liquid flow rate ($C_{NaOH} = 4.0 \text{ mmol L}^{-1}$, $F_g = 0.7 \text{ L min}^{-1}$), (c) concentration of NaOH in R1 ($F_l = 0.49 \text{ ml min}^{-1}$,
 196 $F_g = 0.7 \text{ L min}^{-1}$).

197 3.2 Setting reaction conditions

198 However, precipitates can attach to the wall of the pipeline and LWCC for on-line instruments,
 199 which leads to pipeline blockage and baseline drift. Therefore, we need to optimize reaction conditions,
 200 add the constant temperature module and liquid flow controller temperature to achieve continuous online
 201 measurement of low-concentration ammonia in ambient air. The concentration of the R1 we used in the
 202 initial reaction conditions (longer optical path and smaller sampling volume) contained 1 g L^{-1} salicylic
 203 acid, 0.1 g L^{-1} sodium nitroprusside, and 1 g L^{-1} NaOH. 0.5 ml L^{-1} sodium hypochlorite and 3 g L^{-1} NaOH
 204 were used as R2 (Krom and Michael, 1980; Searle and Phillip, 1984). In addition, the syringe filter was
 205 introduced to minimize the influence of precipitate (Bianchi et al., 2012), but a large drift of the baseline
 206 would still occur during the long time run in our experiment, which will be discussed in detail later. In
 207 fact, we tried interrupting the sampling for a few minutes and implementing 5% hydrochloric acid for
 208 the system to remove these precipitates. However, the concentration changed greatly before and after
 209 each cleaning precipitation. In addition, once the precipitation was formed, it will take a long time to
 210 remove the precipitation, which will also increase the risk of contaminating the detector. According to
 211 reaction kinetics, reducing the stripping and derivatization concentrations (solution concentration) and
 212 $[\text{OH}^-]$ of the system can greatly reduce the formation of precipitates in the solution. Therefore, we need
 213 to find the optimal reaction conditions to produce the least amount of precipitate. The maximum
 214 absorbance of a $100 \text{ } \mu\text{g L}^{-1}$ NH_4^+ standard solution was obtained at $18.75 \text{ mmol L}^{-1}$ OH^- and we could
 215 obtain a high absorbance of light and a slow speed of precipitate formation, which meant that 1.5 g L^{-1}

216 NaOH was added to the derivatization solution, resulted in the precipitate in the solution being too small
 217 to cause pipeline blockage and baseline drift. Importantly, we added regular assessment of the system
 218 drift through use of online sampling of pure N₂. The range of blank signal in continuous operation for 48
 219 h were 2.856 V ~ 2.848 V and 2.254 V ~ 1.834 V of reduced solution concentration and former high
 220 solution concentration, and the maximum offset were 0.3% and 18.6%, respectively, the baseline of low
 221 concentration solution has better stability (Fig. 3). In addition, the concentrations of salicylic acid, sodium
 222 nitroferricyanide and sodium hypochlorite were 0.04, 0.02 and 0.006 times lower than those in previous
 223 research, respectively (Bianchi et al., 2012). In general, the iron-containing precipitate increase the
 224 absorbance by scattering or absorbing light, resulting in measurement bias. In this study, the amount of
 225 iron-containing precipitation is very small by reducing the content of components and alkali of the
 226 solution system, and the voltage of the instrument will not drop significantly due to contamination, which
 227 is conducive to better maintenance of the baseline.



228

229 Fig. 3. The blank time series of the NH₃ detector ran continuously for 48 h. (Low concentration: 0.75 g L⁻¹ salicylic
 230 acid, 0.014 g L⁻¹ sodium nitroferricyanide, and 0.2 g L⁻¹ NaOH as R1, then the 0.188 ml L⁻¹ Sodium hypochlorite and
 231 1.5 g L⁻¹ NaOH as R2; High concentration: 1 g L⁻¹ salicylic acid, 0.1 g L⁻¹ sodium nitroferricyanide, and 1 g L⁻¹
 232 NaOH as R1, then the 0.5 ml L⁻¹ Sodium hypochlorite and 3 g L⁻¹ NaOH as R2).

233 3.3 Stability of liquid flow and temperature

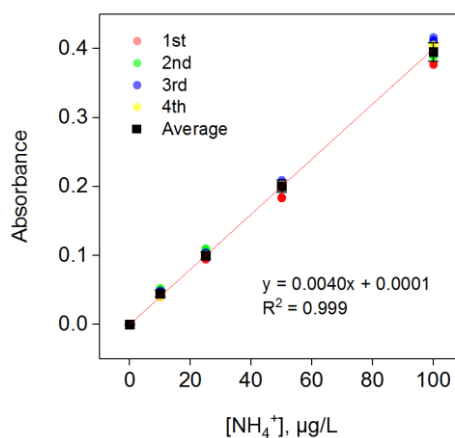
234 The temperature control module and flow control system were designed because of the sensitivity of
 235 molecular absorption spectrophotometry to ambient temperature and residence time. A commercial PID

236 temperature controller was used to control the temperature of the reaction coil with the accuracy of ± 0.1
237 $^{\circ}\text{C}$. The temperature control module was used to control the constant temperature from the reaction coil
238 to LWCC at 55.0 ± 0.1 $^{\circ}\text{C}$. At the same time, the flow control system could control the rotational speed of
239 the peristaltic. This system used a commercialized liquid flow meter (SLI-1000, Sensirion, Switzerland)
240 detect the flow rate and feedback to the peristaltic pump control by detecting the flow of tiny bubbles,
241 which further improved the stability of the reaction process. In other words, the flow control system
242 could avoid the flow rate dropping caused by the abrasion of the pump tube and increase the flow rate
243 caused by the replacement of the pump tube, keeping the R1 flow at a constant set point (0.49 ml min^{-1}).

244 In addition, we designed a buffer tube with a cooling function to further reduce the effects of
245 precipitation. After the derivatization reaction in the reaction coil at 55.0 $^{\circ}\text{C}$, the mixed solution entered
246 the cooling buffer tube. Most of the precipitation was generated in the buffer tube and attached to the
247 tube wall, while some of the precipitation generated in the downstream pipeline was intercepted by an
248 in-line precipitate filter with a pore size of $1.0 \mu\text{m}$ before the LWCC, and the filter was changed weekly.

249 Overall, the above work can make the instrument maintain a relatively stable reaction time and
250 temperature, which can promote a relatively stable reaction process, resulting in a high reproducibility
251 to the same concentration of NH_3 . In the calibration process, R1 was used as diluent, and the
252 concentrations were 10, 25, 50, 75, 100, 150, and $200 \mu\text{g L}^{-1}$ of NH_4^+ standard solution. High purity N_2
253 was used as blank gas into the sampling tube, and the standard solution entered the solution system
254 instead of the R1. Fig. 4 showed the calibration with the NH_4^+ concentration gradient of 0, 10, 25, 50 and
255 $100 \mu\text{g L}^{-1}$ (150, and $200 \mu\text{g L}^{-1}$ of NH_4^+ standard solutions were out of the detection range, which was
256 discussed in section 3.4). Each concentration point was run for 40 minutes, and the relative standard
257 deviation (RSD) calculated from four consecutive measurements (the collection of the four replicates
258 were completed during a 4-week of constant instrument operation) ranged from 0.32 % to 2.65 %, with
259 the k varying from 0.0037 to 0.0040. Moreover, the blank experiment tests were automatically made
260 every one or two days, that is, high purity N_2 was used as a blank gas through the sample tube for 40
261 minutes, the RSD of the blank signal in continuous operation for one month was 1.8 %, which indicated
262 good repeatability and stability of the instrument. Seven switching samples were performed with $50 \mu\text{g}$
263 L^{-1} NH_4^+ standard solution and R1, after calculating 10-90 % of the full signal after a change in

264 concentration, the time response was approximately 140 s, which was much quicker than the method
 265 described by Bianchi et.al (measured to be 10 min) (Bianchi et al., 2012).



266

267

Fig. 4. Calibration curves of standard solution with the same concentration gradient 4 times

268

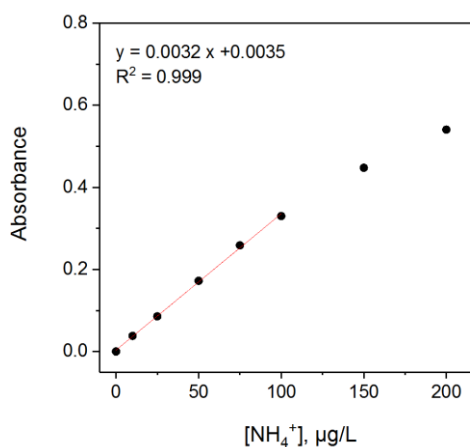
Table 1. Linear regression with the same concentration gradient 4 times

Time	k	b	R ²
1st	0.0037	0.0018	0.9998
2nd	0.0039	0.0046	0.9996
3rd	0.0040	0.0034	0.9997
4th	0.0040	0.0003	0.9999

269 3.4 Setup of the temperature

270 High temperature can accelerate the reaction process and achieve better measurement accuracy and
 271 precision. The voltage signal decreased with increasing temperature; conversely, the absorbance
 272 increased with temperature. According to the flow rate (gas flow rate of 0.70 L min⁻¹, liquid flow rate of
 273 0.49 ml min⁻¹), the detection limit of our SAC-LOPAP can reduce to less than 50 ppt when the absorbance
 274 of 50 µg L⁻¹ NH₄⁺ standard solution reached 0.15 or more. However, if the temperature is too high, there
 275 is a danger that the pipeline interface of the instrument will fall off. Considering the continuous delivery
 276 of solutions (the stability of pipeline connections) and the detection limit (lower than 50 ppt), 55 °C was
 277 selected as the best reaction operating temperature of the instrument, at which sufficient absorbance could
 278 be achieved to detect concentrations of ammonia gas. The standard solution entered the solution system
 279 instead of the stripping solution, then the measured absorbance values were used as absorbance-standard

280 solution concentration plot and regression calculation (The experimental process has been described in
 281 Section 3.3). The result is shown in Fig. 5, a high degree of correlation was found between the standard
 282 solution and absorbance with a correlation coefficient of $R^2 = 0.99$ for the standard solution of 0-100 μg
 283 L^{-1} , however, due to the incomplete reaction of NH_4^+ with dye products, there are two points outside of
 284 the linear fit (standard solution concentrations are 150 and 200 $\mu\text{g L}^{-1}$). Therefore, the approximate
 285 mixing ratio of NH_3 corresponding to the standard liquid concentration is 0-99.1 ppb, which is more
 286 than adequate for monitoring urban areas. The detection limit for NH_4^+ liquid solution is about 40.9 ng
 287 L^{-1} , which is calculated as 3 times the average standard deviation of blank signal noise in one hour. With
 288 an air sample flow rate of 0.7 L min^{-1} and a liquid flow rate of 0.49 ml min^{-1} , this translates to a gas phase
 289 mixing ratio of about 40.5 ppt. In other words, the measurement range was 40.5 ppt up to 99.1 ppb for
 290 NH_3 , which was well suited for the investigation of the NH_3 budget from urban to rural conditions in
 291 China. At the same time, according to the zero point data and the calibration, the corresponding
 292 concentration to the voltage signal of 0.1 mV is 3.1 ppt, which far meets our requirements for actual
 293 environmental measurement. Importantly, the detection limit can be decreased by improving the gas flow.
 294 We can increase our detection range by reducing the reaction temperature and shortening the length of
 295 LWCC. ~~When the temperature drops to 50°C , the range can be up to 200 ppb.~~ We agree with the referee
 296 and we added this sentence in section 3.4 “For example, the following table could be obtained according
 297 to Formula 5 and the stability ranges of F_l and the F_g . The detection limit could be reduced to 14.47 ppt
 298 and the detection upper limit can be increased to 519.02 ppb by adjusting the F_l and the F_g (Table.2)”.
 299



300

301

Fig. 5. Standard solution and absorbance liner range test, to get a measurement range

302

Table 2. Relationship between F_l , F_g and detection range of SAC-LOPAP

$F_l, \text{ml min}^{-1}$	$F_g, \text{L min}^{-1}$	$C(\text{NH}_3)_{\text{min}}, \text{ppt}, [\text{NH}_4^+] = 40.9 \text{ ng L}^{-1}$	$C(\text{NH}_3)_{\text{max}}, \text{ppb}, [\text{NH}_4^+] = 100 \text{ } \mu\text{g L}^{-1}$
<u>0.25</u>	<u>1</u>	<u>14.47</u>	<u>35.38</u>
<u>0.35</u>	<u>0.85</u>	<u>23.84</u>	<u>58.29</u>
<u>0.5</u>	<u>0.7</u>	<u>41.35</u>	<u>101.11</u>
<u>0.75</u>	<u>0.4</u>	<u>108.55</u>	<u>265.41</u>
<u>1.1</u>	<u>0.3</u>	<u>212.28</u>	<u>519.02</u>

303

4. Comparison in urban Beijing

304

305

306

307

308

309

310

311

312

313

314

315

316

317

318

319

320

321

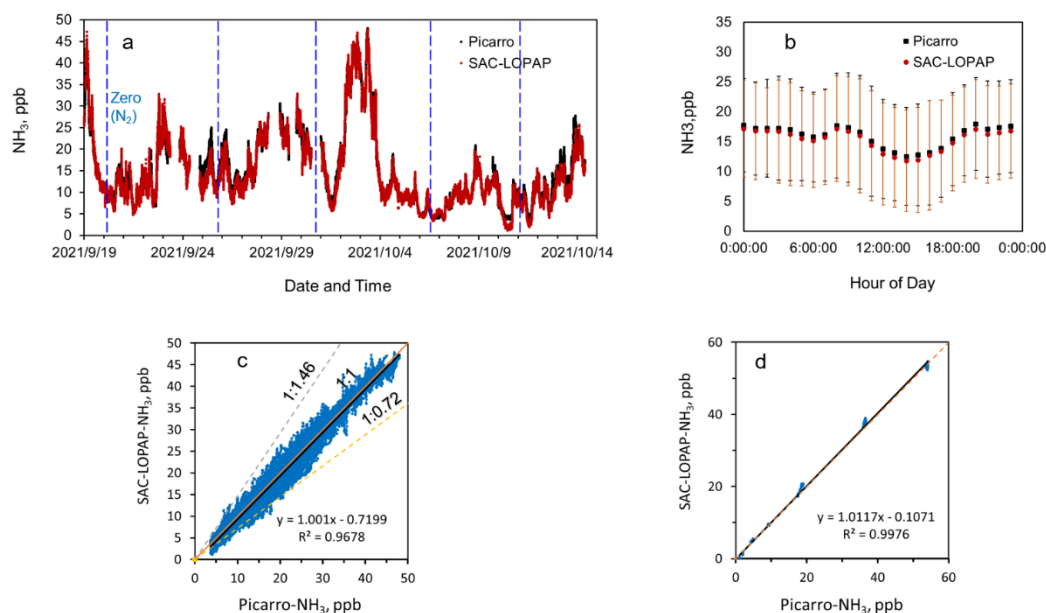
322

323

The time series of the concentration of NH_3 during the inter-comparison period of Picarro and SAC-LOPAP were presented in Fig. 6a. There were a few data gaps for the above instruments caused by calibration operations and instrument maintenance. Instruments display similar temporal features for NH_3 concentrations over the duration of the study. In this study, the concentration of our instrument ranged from 1.3 ppb to 47.86 ppb with an average of 12.64 ± 8.63 ppb, which was close to the concentrations of Picarro (12.76 ± 8.57 ppb). The response speed was similar, indicated that SAC-LOPAP responded in time to rapid changed in NH_3 concentration. The diurnal variation results showed that the concentrations measured by the two instruments were very similar, with our instrument slightly lower than Picarro by 0.72 ppb (Fig. 6b). Furthermore, relatively good correlations for the NH_3 data observed by these instruments were achieved over a large dynamic range of concentration with a slope of 1.00 and an R^2 of 0.96 (Fig. 6c). We found that most of the time there were good correlations between the two instruments within one day except for the data of 23th and 30th September. The regression slope for all the days with higher and lower slopes are 1.46 and 0.72, respectively. We performed in-situ testing of both systems with a cylinder, we produced NH_3 concentrations of about 1.32, 4.95, 9.59, 17.90 and 54.96 ppb. Fig. 6d showed regression analyses of the NH_3 standard gas concentrations obtained with the two instruments. The NH_3 concentrations measured by picarro and our instrument were strongly correlated, with a slope of 1.01 and an R^2 of 0.99.

In general, our instrument run relatively stable with the standard deviation of zero gas during the one month of observations being within 26 ppt (Picarro: 23 ppt), which was far below our detection limit. Furthermore, the drift of SAC-LOPAP and Picarro at 4.95 ppb were 3.5% and 2.8%, while the drifts of

324 54.96 ppb were 1.5% and 0.7%, which meant that our instrument could keep steady for a long time and
 325 it could be used for the continuous online measurement of low concentration of ambient air. More
 326 detailed inter-comparison for these NH₃ instruments will be analyzed in a future publication.
 327



328 Fig. 6. (a) Time series of NH₃ concentration during the comparison, (b) Diurnal variation of NH₃ concentrations
 329 observed by Picarro and SAC-LOPAP, (c) Regression analysis of the NH₃ concentrations observed by Picarro and
 330 SAC-LOPAP, and (d) Regression analysis of different concentrations of Picarro and SAC-LOPAP NH₃ standard
 331 gases.

332 5. Conclusions

333 Ammonia (NH₃) in the atmosphere affects the environment and human health and is therefore
 334 increasingly recognized by policy makers as an important air pollutant that needs to be mitigated. The
 335 accurate and precise detection of ambient NH₃ concentrations is therefore an urgent need for the
 336 exploration of secondary pollution at the regional scale in China.

337 At the present stage, ambient NH₃ measurements at many supersites are still done with spectroscopic,
 338 mass spectrometric and wet chemical methods, which are restricted by the high detection limit and lower
 339 time resolution. In this study, we provide an online NH₃ monitoring system based on wet chemistry
 340 stripping and long path absorption photometer of atmospheric NH₃, our new SAC-LOPAP system has
 341 several significant improvements: one is the optimization of reaction conditions. The low concentration

342 but higher flow rate of solutions decreases the precipitate's production, and the cooling buffer tube and
343 the filter trap most of the precipitates. The others are the constant temperature module and liquid flow
344 controller. The constant temperature module in the system reduces the influence of ambient temperature
345 on the reaction process and color degree. Similarly, adding a liquid flow controller is helpful to the
346 stability of the flow rate and further increases the stability of the reaction process. These improvements
347 reduce the system error and significantly increase the sustainability of SAC-LOPAP operation. Our
348 instrument reached a detection limit of about 40.5 ppt with a stripping liquid flow rate of 0.49 ml min⁻¹
349 and a gas sample flow rate of 0.70 L min⁻¹ in the current condition, and the measuring range of the
350 instrument is ~~40.5 ppt to 99.1~~ 40.5 ppt to 99.1 ppb. Our system has also been characterized in a laboratory setting where
351 we can measure low concentrations. SAC-LOPAP and Picarro were compared in urban areas for a month
352 with relatively good agreement ($R^2 = 0.967$). In addition, the diurnal variation results showed that the
353 concentrations of the two instruments were very similar. Therefore, we conclude that our update of the
354 ammonia measurement experimental framework has been successful. However, more research about
355 field measurement and comparison is needed to verify the equipment's performance in routine
356 observation, and the influence of particulate ammonium on the results of NH₃ detection also requires
357 further study.

358

359 **Data availability.** The datasets used in this study are available from the corresponding author upon
360 request (hbdong@pku.edu.cn).

361

362 **Author contributions.** H.B.D. designed the study. S.S.T., K.X.Z. set up and characterized the instrument,
363 analyzed the data and wrote the paper with the input of H.B.D. As co-authors, S.S.T and K.X.Z.
364 contributed equally to this paper. All authors contributed to the field measurements, discussed and
365 improved the paper.

366

367 **Competing interests.** The authors declare that they have no conflict of interest.

368

369 **Acknowledgments.** This work was supported by special fund of State Key Joint Laboratory of
370 Environmental Simulation and Pollution Control (Grants No.22Y04ESPCP)

371

372 **References.**

- 373 Ajay and Beniwal.: Electrospun SnO₂/PPy nanocomposite for ultra-low ammonia concentration detection at room
374 temperature, *Sensors & Actuators B Chemical*, 296, 126660.1-126660.9, <https://doi.org/10.1016/j.snb.2019.126660>,
375 2019.
- 376 Bae, M. S., Demerjian, K. L., Schwab, J. J., Weimer, S., Hou, J., Zhou, X., Rhoads, K., and Orsini, D.:
377 Intercomparison of Real Time Ammonium Measurements at Urban and Rural Locations in New York, *Aerosol*
378 *Science & Technology*, 41, 329-341, <https://doi.org/10.1080/02786820701199710>, 2007.
- 379 Behera, S. N., Sharma, M., Aneja, V. P., and Balasubramanian, R.: Ammonia in the atmosphere: a review on
380 emission sources, atmospheric chemistry and deposition on terrestrial bodies, *Environ Sci Pollut Res Int*, 20, 8092-
381 8131, <https://doi.org/10.1007/s11356-013-2051-9> 2013.
- 382 Benson, D. R., Markovich, A., Al-Refai, M., and Lee, S. H.: A Chemical Ionization Mass Spectrometer for ambient
383 measurements of Ammonia, *Atmos. Meas. Tech.*, 3, 1075-1087, <https://doi.org/10.5194/amt-3-1075-2010>, 2010.
- 384 Berden, G., Peeters, R., Meijer, G., and Apituley, A.: Open-path trace gas detection of ammonia based on cavity-
385 enhanced absorption spectroscopy, *Applied Physics B* 71, 231-216, <https://doi.org/10.1007/s003400000302>, 2000.
- 386 Bianchi, F., Dommen, J., Mathot, S., and Baltensperger, U.: On-line determination of ammonia at low pptv mixing
387 ratios in the CLOUD chamber, *Atmospheric Measurement Techniques*, 5, 1719-1725,
388 <https://doi.org/10.5194/amt-5-1719-2012>, 2012.
- 389 Bu, X., Xie, Z., Liu, J., Wei, L., and Ren, H.: Global PM_{2.5}-attributable health burden from 1990 to 2017: estimates
390 from the Global Burden of Disease Study 2017, *Environmental Research*, 197, 111123,
391 <https://10.1016/j.envres.2021.111123>, 2021.
- 392 Callahan, M. R., Rose, J. B., and Byrne, R. H.: Long pathlength absorbance spectroscopy: trace copper analysis
393 using a 4.4 m liquid core waveguide, *Talanta*, 58, 891-898, [https://doi.org/10.1016/S0039-9140\(02\)00403-4](https://doi.org/10.1016/S0039-9140(02)00403-4) 2002.
- 394 Chen, X., Oro, Y., Tanaka, K., Takenaka, N., and Bandow, H.: A New Method for Atmospheric Nitrogen Dioxide
395 Measurements Using the Combination of a Stripping Coil and Fluorescence Detection, *Analytical Sciences the*
396 *International Journal of the Japan Society for Analytical Chemistry*, 20, 1019-1023,
397 <https://doi.org/10.2116/analsci.20.1019>, 2004.
- 398 Dong, H. B., Zeng, L. M., Hu, M., Wu, Y. S., Zhang, Y. H., Slanina, J., Zheng, M., Wang, Z. F., and Jansen, R.:
399 Technical Note: The application of an improved gas and aerosol collector for ambient air pollutants in China,
400 *ATMOSPHERIC CHEMISTRY AND PHYSICS*, 12, 10519-10533, <https://doi.org/10.5194/acp-12-10519-2012>,
401 2012.
- 402 Fowler, D., Steadman, C. E., Stevenson, D., Coyle, M., Rees, R. M., Skiba, U. M., Sutton, M. A., Cape, J. N., Dore,
403 A. J., and Vieno, M.: Effects of global change during the 21st century on the nitrogen cycle, *Atmospheric chemistry*
404 *and physics*, 15, 13849-13893, <https://doi.org/10.5194/acp-15-13849-2015>, 2015.
- 405 Gao, X., Koutrakis, P., Coull, B., Lin, X., Vokonas, P., Schwartz, J., and Baccarelli, A. A.: Short-term exposure to
406 PM_{2.5} components and renal health: Findings from the Veterans Affairs Normative Aging Study, *Journal of*
407 *Hazardous Materials*, 420, 126557, <https://10.1016/j.jhazmat.2021.126557>, 2021.
- 408 Gong, D., Liucheng, L. I., Baozeng, L. I., Liping, D., Wang, Y., Yanhua, M. A., Zhang, Z., and Jin, Y.: NH₃
409 measurement based on cavity enhanced absorption spectroscopy, *Laser Technology*, 5, 664-668,
410 <https://doi.org/10.7510/jgjs.issn.1001-3806.2017.05.009>, 2017.
- 411 Heland, J., Kleffmann, J., Kurtenbach, R., and Wiesen, P.: A new instrument to measure gaseous nitrous acid (HONO)
412 in the atmosphere, *Environmental Science & Technology*, 35, 3207-3212, 2001.

413 Ianniello, A., Spataro, F., Esposito, G., Allegrini, I., Hu, M., and Zhu, T.: Chemical characteristics of inorganic
414 ammonium salts in PM_{2.5} in the atmosphere of Beijing (China), *Atmospheric Chemistry & Physics*, 11, 10803-
415 10822, <https://doi.org/10.5194/acp-11-10803-2011>, 2011.

416 Janson, R., Rosman, K., Karlsson, A., and H.-C.HANSSON: Biogenic emissions and gaseous precursors to forest
417 aerosols, *Tellus*, 53, 423-440, <https://doi.org/10.1034/j.1600-0889.2001.d01-30.x>, 2010.

418 Khlystov, A., Wyers, G. P., Brink, H., and Slanina, J.: The steam-jet aerosol collector (SJAC), *Journal of Aerosol*
419 *Science*, 26, S111-S112, [https://doi.org/10.1016/0021-8502\(95\)96963-8](https://doi.org/10.1016/0021-8502(95)96963-8) 1995.

420 Kleffmann, J., Heland, J., Kurtenbach, R., Lrzer, J. C., and Wiesen, P.: A new instrument (LOPAP) for the detection
421 of nitrous acid (HONO), *Environmental Science and Pollution Research*, 9, 48-54, 2002.

422 Klimczyk, M., Siczek, A., and Schimmelpfennig, L.: Improving the efficiency of urea-based fertilization leading to
423 reduction in ammonia emission, *Science of The Total Environment*, 771, 145483,
424 <https://doi.org/10.1016/j.scitotenv.2021.145483>, 2021.

425 Krom and Michael, D.: Spectrophotometric determination of ammonia: a study of a modified Berthelot reaction
426 using salicylate and dichloroisocyanurate, *Analyst*, 105, 305-316, <https://doi.org/10.1039/an9800500305>, 1980.

427 Krupa, S. V.: Effects of atmospheric ammonia (NH₃) on terrestrial vegetation: a review, *Environmental Pollution*,
428 124, 179-221, [https://doi.org/10.1016/S0269-7491\(02\)00434-7](https://doi.org/10.1016/S0269-7491(02)00434-7) 2003.

429 Makkonen, U., Virkkula, A., Mantykentta, J., Hakola, H., Keronen, P., Vakkari, V., and Aalto, P. P.: Semi-
430 continuous gas and inorganic aerosol measurements at a Finnish urban site: comparisons with filters, nitrogen in
431 aerosol and gas phases, and aerosol acidity, *Atmospheric Chemistry and Physics*, 12, 5617-5631,
432 <https://doi.org/10.5194/acp-12-5617-2012>, 2012.

433 Martin, N. A., Ferracci, V., Cassidy, N., and Hoffnagle, J. A.: The application of a cavity ring-down spectrometer to
434 measurements of ambient ammonia using traceable primary standard gas mixtures, *Applied Physics B*, 122, 219,
435 <https://doi.org/10.1007/s00340-016-6486-9>, 2016.

436 Mcmanus, J. B., Nelson, D. D., Shorter, J. H., Zahniser, M. S., and Faist, J.: Quantum cascade lasers for open- and
437 closed-path measurement of trace gases, *Society of Photo-Optical Instrumentation Engineers (SPIE) Conference*
438 *Series*, 4817, <https://doi.org/10.1117/12.452093> 2002.

439 Ni, Ji-Qin, Heber, Albert, J., Lim, Teng, T., Diehl, and Claude: Ammonia Emission from a Large Mechanically-
440 Ventilated Swine Building during Warm Weather, *Journal of Environment Quality*, 29, 751-751,
441 <https://doi.org/10.2134/jeq2000.00472425002900030010x>, 2000.

442 Nowak, J. B., Neuman, J. A., Kozai, K., Huey, L. G., Tanner, D. J., Holloway, J. S., Ryerson, T. B., Frost, G. J.,
443 McKeen, S. A., and Fehsenfeld, F. C.: A chemical ionization mass spectrometry technique for airborne
444 measurements of ammonia, *Journal of Geophysical Research-Atmospheres*, 112,
445 <https://doi.org/10.1029/2006jd007589>, 2007.

446 Qu, Z. C., Li, B. C., and Han, Y. L.: Cavity ring-down spectroscopy for trace ammonia detection, *Journal of Infrared*
447 *& Millimeter Waves*, 31, 431-436, <https://doi.org/10.3724/SP.J.1010.2012.00431>, 2012.

448 Searle and Phillip, L.: The berthelot or indophenol reaction and its use in the analytical chemistry of nitrogen. A
449 review, *Analyst*, 109, 549-540, <https://doi.org/10.1039/an9840900549>, 1984.

450 Sharma, S. K., Datta, A., Saud, T., Saxena, M., Mandal, T. K., Ahammed, Y. N., and Arya, B. C.: Seasonal variability
451 of ambient NH₃, NO, NO₂ and SO₂ over Delhi, *Journal of Environmental Sciences*, 22, 1023-1028,
452 [https://doi.org/10.1016/S1001-0742\(09\)60213-8](https://doi.org/10.1016/S1001-0742(09)60213-8) 2010.

453 Sharma, S. K., Singh, A. K., Saud, T., Mandal, T. K., Saxena, M., Singh, S., Ghosh, S. K., and Raha, S.: Measurement
454 of ambient NH₃ over Bay of Bengal during W_ICARB Campaign, *Annales Geophysicae*, 30, 371-377,
455 <https://doi.org/10.5194/angeo-30-371-2012>, 2012.

456 Sutton, M. A., Fowler, D., Burkhardt, J. K., and Milford, C.: Vegetation atmosphere exchange of ammonia: canopy
457 cycling and the impacts of elevated nitrogen inputs, *Water Air & Soil Pollution*, 85, 2057-2063,
458 <https://doi.org/10.1007/BF01186137> 1995.

459 Swati, A. and Hait, S.: Greenhouse Gas Emission During Composting and Vermicomposting of Organic Wastes –
460 A Review, *CLEAN - Soil Air Water*, 46, 1700042.1-1700042. 3, <https://doi.org/10.1002/clen.201700042>, 2018.

461 Twigg, M. M., Berkhout, A. J. C., Cowan, N., Crunaire, S., Dammers, E., Ebert, V., Gaudion, V., Haaima, M., Häni,
462 C., John, L., Jones, M. R., Kamps, B., Kentisbeer, J., Kupper, T., Leeson, S. R., Leuenberger, D., Lüttschwager, N.
463 O. B., Makkonen, U., Martin, N. A., Missler, D., Mounsor, D., Neftel, A., Nelson, C., Nemitz, E., Oudwater, R.,
464 Pascale, C., Petit, J. E., Pogany, A., Redon, N., Sintermann, J., Stephens, A., Sutton, M. A., Tang, Y. S., Zijlmans,
465 R., Braban, C. F., and Niederhauser, B.: Intercomparison of in situ measurements of ambient NH₃: instrument
466 performance and application under field conditions, *Atmos. Meas. Tech.*, 15, 6755-6787,
467 <https://doi.org/10.5194/amt-15-6755-2022>, 2022.

468 Von, B. K., Braban, C. F., Famulari, D., Jones, S. K., Blackall, T., Smith, T., Blom, M., Coe, H., Gallagher, M., and
469 Ghalaieny, M.: Field inter-comparison of eleven atmospheric ammonia measurement techniques, *Atmospheric*
470 *Measurement Techniques*, 3, 91-112, <https://doi.org/10.5194/amt-3-91-2010>, 2009.

471 Wang, Ruyu, Ye, Xingnan, Liu, Yuxuan, Li, Haowen, Yang, and Xin: Characteristics of atmospheric ammonia and
472 its relationship with vehicle emissions in a megacity in China, *Atmospheric Environment*, 182, 97-104,
473 <https://doi.org/10.1016/j.atmosenv.2018.03.047>, 2018.

474 Wang, Y., Zhang, Q. Q., He, K., Zhang, Q., and Chai, L.: Sulfate-nitrate-ammonium aerosols over China: response
475 to 2000–2015 emission changes of sulfur dioxide, nitrogen oxides, and ammonia, *Atmospheric Chemistry and*
476 *Physics*, 13, 2635-2652 <https://doi.org/10.5194/acp-13-2635-2013>, 2013.

477 Wen, Liang, Xue, Likun, Wang, Xinfeng, Xu, Caihong, Chen, and Tianshu: Summertime fine particulate nitrate
478 pollution in the North China Plain: increasing trends, formation mechanisms and implications for control policy,
479 *Atmospheric Chemistry & Physics*, 18, 11261-11275, <https://doi.org/10.5194/acp-2018-89>, 2018.

480 Whitehead, J. D., Twigg, M., Famulari, D., Nemitz, E., Sutton, M. A., Gallagher, M. W., and Fowler, D.: Evaluation
481 of Laser Absorption Spectroscopy Techniques for Eddy Covariance Flux Measurements of Ammonia,
482 *Environmental Science & Technology*, 42, 2041-2046, <https://doi.org/10.1021/es071596u>, 2008.

483 Yao, W., Byrne, R. H., and Waterbury, R. D.: Determination of Nanomolar Concentrations of Nitrite and Nitrate in
484 Natural Waters Using Long Path Length Absorbance Spectroscopy, *Environmental Science and Technology*, 32,
485 2646-2649, <https://doi.org/10.1021/es9709583> 1998.

486 Yokelson, R., Christian, T., Bertschi, I., and Hao, W.: Evaluation of adsorption effects on measurements of ammonia,
487 acetic acid, and methanol, *Journal of Geophysical Research Atmospheres*, 108,
488 <https://doi.org/10.1029/2003JD003549>, 2003.

489 Yu, H. and Lee, S. H.: Chemical ionisation mass spectrometry for the measurement of atmospheric amines,
490 *Environmental Chemistry*, 9, 190-201, <https://doi.org/10.1029/2003JD00354910.1071/en12020>, 2012.

491